J|A|C|S
ARTICLES
Published on Web 07/02/2005

Why Are BINOL-Based Monophosphites Such Efficient Ligands in Rh-Catalyzed Asymmetric Olefin Hydrogenation?

Manfred T. Reetz,*,† Andreas Meiswinkel,† Gerlinde Mehler,† Klaus Angermund,† Martin Graf,† Walter Thiel,† Richard Mynott,† and Donna G. Blackmond‡

Contribution from the Max-Planck-Institut für Kohlenforschung, Kaiser-Wilhelm-Platz 1, D-45470 Mülheim/Ruhr, Germany, and Department of Chemistry, Imperial College, London SW7 2AZ, U.K.

Received March 30, 2005; E-mail: reetz@mpi-muelheim.mpg.de

Abstract: Whereas recent synthetic studies concerning Rh-catalyzed olefin hydrogenation based on BINOL-derived monodentate phosphites have resulted in an efficient and economically attractive preparative method, very little is known concerning the source of the unexpectedly high levels of enantioselectivity (ee often 90−99%). The present mechanistic study, which includes the NMR characterization of the precatalysts, kinetic measurements with focus on nonlinear effects, and DFT calculations, constitutes a first step in understanding this hydrogenation system. The two most important features which have emerged from these efforts are the following: (1) two monodentate P-ligands are attached to rhodium, and (2) the lock-and-key mechanism holds, in which the thermodynamics of Rh/olefin complexation with formation of the major and minor diastereomeric intermediates dictates the stereochemical outcome. The major diastereomer leads to the favored enantiomeric product, which is opposite to the state of affairs in classical Rh-catalyzed olefin hydrogenation based on chiral chelating diphosphines (anti lock-and-key mechanism as proposed by Halpern).

Introduction

Asymmetric transition-metal-catalyzed olefin hydrogenation dates back to 1968, when Horner[1] and Knowles[2] independently described the first enantioselective versions of Wilkinson's catalyst using chiral monophosphines. The initial enantiomeric excess (ee) values (∼15%) were low by today's standards, but a revolutionary step had been taken. Although several other monodentate phosphines led to higher ee's with certain olefins, it was not until a few years later that a truly important advancement was announced independently by Kagan[3] and Knowles,[4,5] namely the demonstration that highly improved enantioselectivities can be achieved if chiral chelating diphosphines are used as ligands. Shortly thereafter, Noyori[6,7] described the synthesis of one of the most general bidentate ligands known in asymmetric hydrogenation and in a multitude of other transition-metal-catalyzed reactions: BINAP. Since then a variety of other efficient chiral diphosphines have been prepared.[8] Although the respective structure, synthetic effort (i.e., cost), and efficiency in catalysis differ, these ligands are all bidentate. This led to the long-standing dogma that, in general, chelation is necessary in order to achieve high enantioselectivity.[7−11] It is widely accepted that chelation reduces the degree

† Max-Planck-Institut für Kohlenforschung.
‡ Imperial College.

(1) Horner, L.; Siegel, H.; Büthe, H. *Angew. Chem.* **1968**, *80*, 1034−1035; *Angew. Chem., Int. Ed. Engl.* **1968**, *7*, 942−943.
(2) Knowles, W. S.; Sabacky, M. J. *Chem. Commun. (Cambridge, U.K.)* **1968**, 1445−1446.
(3) Dang, T. P.; Kagan, H. B. *J. Chem. Soc. D* **1971**, 481.
(4) Knowles, W. S.; Sabacky, M. J.; Vineyard, B. D.; Weinkauff, D. J. *J. Am. Chem. Soc.* **1975**, *97*, 2567−2568.
(5) Knowles, W. S. *Angew. Chem.* **2002**, *114*, 2096−2107; *Angew. Chem., Int. Ed.* **2002**, *41*, 1998−2007.
(6) Miyashita, A.; Yasuda, A.; Takaya, H.; Toriumi, K.; Ito, T.; Souchi, T.; Noyori, R. *J. Am. Chem. Soc.* **1980**, *102*, 7932−7934.
(7) Noyori, R. *Angew. Chem.* **2002**, *114*, 2108−2123; *Angew. Chem., Int. Ed.* **2002**, *41*, 2008−2022.
(8) Selected papers and reviews of asymmetric olefin hydrogenation:[5, 7] (a) Noyori, R. *Chem. Soc. Rev.* **1989**, *18*, 187−208. (b) Heller, D.; Thede, R.; Haberland, D. *J. Mol. Catal. A* **1997**, *115*, 273−281. (c) Bircher, H.; Bender, B. R.; von Philipsborn, W. *Magn. Reson. Chem.* **1993**, *31*, 293−298. (d) Gridnev, I. D.; Yamanoi, Y.; Higashi, N.; Tsuruta, H.; Yasutake, M.; Imamoto, T. *Adv. Synth. Catal.* **2001**, *343*, 118−136. (e) Gridnev, I. D.; Imamoto, T. *Acc. Chem. Res.* **2004**, *37*, 633−644. (f) Crépy, K. V. L.; Imamoto, T. *Adv. Synth. Catal.* **2003**, *345*, 79−101. (g) Blaser, H.-U.; Malan, C.; Pugin, B.; Spindler, F.; Steiner, H.; Studer, M. *Adv. Synth. Catal.* **2003**, *345*, 103−151. (h) Tang, W.; Zhang, X. *Chem. Rev.* **2003**, *103*, 3029−3069. (i) Saluzzo, C.; Lemaire, M. *Adv. Synth. Catal.* **2002**, *344*, 915−928. (j) Dwars, T.; Oehme, G. *Adv. Synth. Catal.* **2002**, *344*, 239−260. (k) Jeulin, S.; Duprat de Paule, S.; Ratovelomanana-Vidal, V.; Genêt, J.-P.; Champion, N.; Dellis, P. *Proc. Natl. Acad. Sci. U.S.A.* **2004**, *101*, 5799−5804.
(9) (a) Chan, A. S. C.; Pluth, J. J.; Halpern, J. *J. Am. Chem. Soc.* **1980**, *102*, 5952−5954. (b) Halpern, J. *Science* **1982**, *217*, 401−407. (c) Landis, C. R.; Halpern, J. *J. Am. Chem. Soc.* **1987**, *109*, 1746−1754. (d) McCulloch, B.; Halpern, J.; Thompson, M. R.; Landis, C. R. *Organometallics* **1990**, *9*, 1392−1395. (e) Halpern, J. In *Chiral Catalysis*; Morrison, J. D., Ed.; Academic Press: Orlando, FL, 1985; Vol. 5, pp 41−69. (f) Halpern, J.; Riley, D. P.; Chan, A. S. C.; Pluth, J. J. *J. Am. Chem. Soc.* **1977**, *99*, 8055−8057.
(10) (a) Brown, J. M.; Chaloner, P. A. *J. Am. Chem. Soc.* **1980**, *102*, 3040−3048. (b) Brown, J. M.; Evans, P. L.; Lucy, A. R. *J. Chem. Soc., Perkin Trans. 2* **1987**, 1589−1596. (c) Brown, J. M.; Evans, P. L. *Tetrahedron* **1988**, *44*, 4905−4916. (d) Brown, J. M.; Rose, M.; Knight, F. I.; Wienand, A. *Recl. Trav. Chim. Pays-Bas* **1995**, *114*, 242−251. (e) Brown, J. In *Comprehensive Asymmetric Catalysis*; Jacobsen, E. N., Pfaltz, A., Yamamoto, H., Eds.; Springer: Berlin, 1999; Vol. 5, Chapter 5.1.
(11) (a) Landis, C. R.; Hilfenhaus, P.; Feldgus, S. *J. Am. Chem. Soc.* **1999**, *121*, 8741−8754. (b) Feldgus, S.; Landis, C. R. *J. Am. Chem. Soc.* **2000**, *122*, 12714−12727. (c) Landis, C. R.; Feldgus, S. *Angew. Chem.* **2000**, *112*, 2985−2988; *Angew. Chem., Int. Ed.* **2000**, *39*, 2863−2866. (d) Feldgus, S.; Landis, C. R. *Organometallics* **2001**, *20*, 2374−2386.

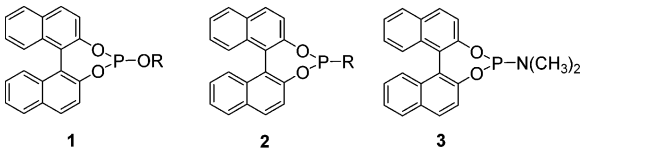

Figure 1. Monodentate P-ligands useful in Rh-catalyzed olefin hydrogenation.

of rotational freedom around the metal−phosphorus bond, leading to a certain degree of rigidity necessary for efficient transfer of chirality in the catalytic process.

Parallel to these developments, the mechanism of Rh-catalyzed asymmetric olefin hydrogenation was studied by several groups.[7−11] In a series of classic papers, Halpern showed that the difference in thermodynamic stability of the two diastereomeric Rh/substrate intermediates arising from the π-complexation of the two enantiotopic faces of an α-acylamino acrylate serving as the prochiral olefin is not the cause of enantioselectivity.[9] Rather, the minor diastereomer reacts faster than the major intermediate (anti lock-and-key postulate). Later, Landis carried out theoretical calculations which support this.[11] However, the Halpern postulate was never claimed to be general. Genêt was the first to postulate an exception, although detailed mechanistic evidence remains to be presented.[12] A stronger case for the lock-and-key postulate was made by Evans, who used P,S-ligands in the Rh-catalyzed hydrogenation of α-acylamino acrylates.[13] Most recently, Heller has published compelling evidence for anti-Halpern behavior in the Rh-catalyzed hydrogenation of β-acylamino acrylates using traditional chiral diphosphines.[14] It thus appears that the nature of the bidentate ligands and the type of substrate determine whether a Halpern or anti-Halpern system pertains.

In 2000, three groups independently reported that certain BINOL-based *monodentate* phosphorus compounds are excellent ligands in Rh-catalyzed olefin hydrogenation, namely phosphites (**1**),[15] phosphonites (**2**),[16] and phosphoramidites (**3**)[17] (Figure 1). In many cases the enantioselectivity of Rh-catalyzed olefin hydrogenation was found to range between 90% and 99% ee, which came as a surprise because chelation is not possible in these systems.

There are several reasons why industrial and academic interest in this new chapter of asymmetric hydrogenation has increased enormously during the past five years.[18,19] BINOL (**4**) is commercially available in both enantiomeric forms and is one of the cheapest chiral auxiliaries currently on the market. Moreover, the ligands **1**−**3** are readily available. For example, transformation of BINOL into modular phosphites (**1**) requires only two simple steps, and a multitude of readily accessible achiral or chiral alcohols **6** can serve as the second component. This means that the search for the optimal ligand in the asymmetric hydrogenation of a given substrate is empirical. Finally, phosphites are much less prone to suffer undesired oxidation than phosphines.

Table 1. Rh-Catalyzed Hydrogenation of **7** Using Monophosphites **1** as Ligands

entry	ligand	ee (%)	entry	ligand	ee (%)
1	**1a**	89.2	7	**1g**	96.6
2	**1b**	93.4	8	**1h**	98.2
3	**1c**	97.6	9	**1i**	96.0
4	**1d**	91.4	10	**1j**	89.8
5	**1e**	98.6	11	**1k**	39.2
6	**1f**	96.8	12	**1l**	28.6

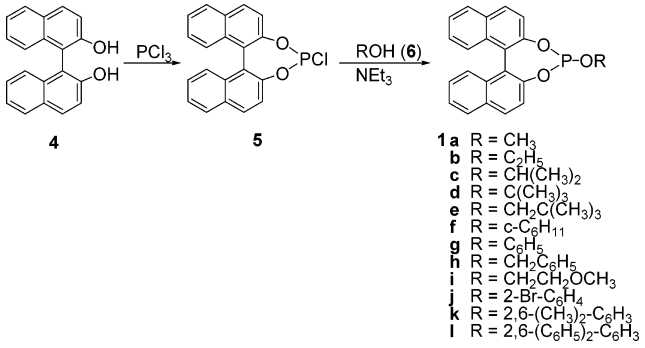

In our original work, we demonstrated that the nature of the group R in the modular ligand **1** has a crucial influence on the degree of enantioselectivity in a given hydrogenation reaction.[15,18] An example is the Rh-catalyzed hydrogenation of itaconic acid dimethyl ester (**7**). Table 1 summarizes a portion of our data which shows that the ee can vary between 28% and 99%, depending solely upon the nature of the group R in the monodentate ligand **1**.

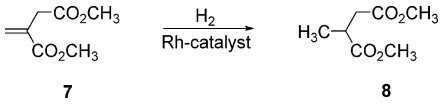

Since then, we[18] and other groups[20] have generalized on these findings, studying other types of olefins and other BINOL-derived compounds **1** or related monodentate phosphites which

(12) (a) Marinetti, A.; Jus, S.; Genêt, J.-P. *Tetrahedron Lett.* **1999**, *40*, 8365−8368. (b) Genêt, J.-P.; Marinetti, A.; Ratovelomanana-Vidal, V. *Pure Appl. Chem.* **2001**, *73*, 299−303.

(13) Evans, D. A.; Michael, F. E.; Tedrow, J. S.; Campos, K. R. *J. Am. Chem. Soc.* **2003**, *125*, 3534−3543.

(14) Drexler, H.-J.; Baumann, W.; Schmidt, T.; Zhang, S.; Sun, A.; Spannenberg, A.; Fischer, C.; Buschmann, H.-J.; Heller, D. *Angew. Chem.* **2005**, *117*, 1208−1212; *Angew. Chem., Int. Ed.* **2005**, *44*, 1184−1188.

(15) (a) Reetz, M. T.; Mehler, G. *Angew. Chem.* **2000**, *112*, 4047−4049; *Angew. Chem., Int. Ed.* **2000**, *39*, 3889−3890. (b) Reetz, M. T.; Mehler, G.; Meiswinkel, A. Patent WO 01/94278 A1, 2001.

(16) (a) Reetz, M. T.; Sell, T. *Tetrahedron Lett.* **2000**, *41*, 6333−6336. (b) Claver, C.; Fernandez, E.; Gillon, A.; Heslop, K.; Hyett, D. J.; Martorell, A.; Orpen, A. G.; Pringle, P. G. *Chem. Commun. (Cambridge, U.K.)* **2000**, 961−962.

(17) Van den Berg, M.; Minnaard, A. J.; Schudde, E. P.; van Esch, J.; de Vries, A. H. M.; de Vries, J. G.; Feringa, B. L. *J. Am. Chem. Soc.* **2000**, *122*, 11539−11540.

(18) (a) Reetz, M. T.; Mehler, G.; Meiswinkel, A.; Sell, T. *Tetrahedron Lett.* **2002**, *43*, 7941−7943. (b) Reetz, M. T. *Chim. Oggi* **2003**, *21* (10/11), 5−8. (c) Reetz, M. T. *Russ. J. Org. Chem.* **2003**, *39*, 392−396. (d) Reetz, M. T.; Goossen, L. J.; Meiswinkel, A.; Paetzold, J.; Feldthusen Jensen, J. *Org. Lett.* **2003**, *5*, 3099−3101. (e) Reetz, M. T. In *Comprehensive Coordination Chemistry II*; Ward, M. D., Ed.; University of Bristol: Bristol, U.K., 2004; Vol. 9, pp 509−548. (f) Reetz, M. T.; Ma, J.-A.; Goddard, R. *Angew. Chem.* **2005**, *117*, 416−419; *Angew. Chem., Int. Ed.* **2005**, *44*, 412−415.

(19) (a) Minnaard, A. J.; van den Berg, M.; Schudde, E. P.; van Esch, J.; de Vries, A. H. M.; de Vries, J. G.; Feringa, B. L. *Chim. Oggi* **2001**, *19*, 12−13. (b) Van den Berg, M.; Minnaard, A. J.; Haak, R. M.; Leeman, M.; Schudde, E. P.; Meetsma, A.; Feringa, B. L.; de Vries, A. H. M.; Maljaars, C. E. P.; Willans, C. E.; Hyett, D.; Boogers, J. A. F.; Henderickx, H. J. W.; de Vries, J. G. *Adv. Synth. Catal.* **2003**, *345*, 308−323. (c) Peña, D.; Minnaard, A. J.; de Vries, J. G.; Feringa, B. L. *J. Am. Chem. Soc.* **2002**, *124*, 14552−14553. (d) Bernsmann, H.; van den Berg, M.; Hoen, R.; Minnaard, A. J.; Mehler, G.; Reetz, M. T.; de Vries, J. G.; Feringa, B. L. *J. Org. Chem.* **2005**, *70*, 943−951. (e) Wu, S.; Zhang, W.; Zhang, Z.; Zhang, X. *Org. Lett.* **2004**, *6*, 3565−3567. (f) For a monodentate phosphoramidite derived from a spiro-diol, see: Hu, A.-G.; Fu, Y.; Xie, J.-H.; Zhou, H.; Wang, L.-X.; Zhou, Q.-L. *Angew. Chem.* **2002**, *114*, 2454−2456; *Angew. Chem., Int. Ed.* **2002**, *41*, 2348−2350.

incorporate a variety of achiral and chiral alcohols (including carbohydrate alcohols) as additional building blocks. In addition to studying the scope and limitation of this new method, it was desirable to illuminate the reason(s) for high enantioselectivity in these hydrogenation reactions. In this paper, we focus on mechanistic studies which address the NMR spectra of the Rh complexes, the reaction kinetics, nonlinear effects (NLE), and density functional theory (DFT) calculations.

NMR Spectroscopic Characterization of the Phosphites and the Rh Complexes

All of the monodentate phosphites **1** were characterized by ^{1}H, ^{13}C, and ^{31}P NMR spectroscopy.[21] The NMR spectra are fully consistent with the given structures. A detailed NMR study of **1e** (R = neopentyl) was performed in order to interpret the spectra of the other phosphites (Experimental Section). The naphthyl groups are diastereotopic, and therefore all the protons and carbon nuclei within them are inequivalent. The ^{1}H and ^{13}C NMR signals are all resolved, with the exception of C3/C3′. Upon combining the known Rh complex $[Rh(cod)_2]BF_4$ (cod = 1,5-cyclooctadiene) (**9**) with 2 equiv of a monodentate phosphite **1**, a smooth reaction occurred in which one of the cod ligands is replaced by two phosphite ligands, with formation of the precatalysts **10**:

$$\underset{\mathbf{9}}{Rh(cod)_2BF_4} + 2\,\mathbf{1} \rightarrow \underset{\mathbf{10}}{Rh(\mathbf{1})_2(cod)_2BF_4} + cod$$

We have characterized a number of these Rh compounds by ^{1}H, ^{13}C, and ^{31}P NMR spectroscopy, and we present here the data of the neopentyl phosphite-derived complex **10e**. A single phosphorus signal was observed, a doublet as a result of spin−spin coupling with ^{103}Rh (100%), centered at 120.8 ppm. The stoichiometry of the RhL_2(cod) complex was confirmed by the integrated intensities in the ^{1}H NMR spectrum, in line with the fine structure of the multiplets of the olefinic carbon atoms of the cod ligand. Consistent with the ^{31}P NMR spectrum, just one set of signals is observed in the ^{1}H and ^{13}C NMR spectra for the two phosphite ligands. This shows that the phosphite ligands are, as expected, symmetrically equivalent. However, as in the free ligand, the naphthyl groups are inequivalent (diastereotopic). For the cod ligand, four signals are observed in the ^{13}C NMR spectrum. While the complexed double bonds are identical, within each double bond the carbon atoms are diastereotopic (109.4 and 109.1 ppm). As expected, two methylene ^{13}C signals are observed (30.9 and 28.8 ppm).

Kinetics

Kinetic studies of asymmetric olefin hydrogenation provide valuable insight into the mechanism of this catalytic process.[5,7−10,22] Moreover, the determination of relative reaction rates arising from two or more catalysts is important for practical reasons. In an initial experiment, we compared the rate of hydrogenation of itaconic acid diester **7** using the isopropyl phosphite-derived catalyst $Rh(\mathbf{1c})_2(cod)BF_4$ (**10c**) and the standard BINAP-based system Rh(BINAP)(cod)BF_4. Monitoring of H_2 uptake as a function of time served as a measure of activity at a substrate-to-catalyst ratio of 20000 and a pressure (H_2) of 5 bar. Figure 2 reveals that the two systems differ considerably in their activity, with the phosphite-based catalyst being significantly more active than the BINAP system. GC monitoring corroborated this conclusion, showing that in the former case conversion is complete within 8 min, whereas the BINAP-derived catalyst requires more than 1000 min for only 55% conversion.

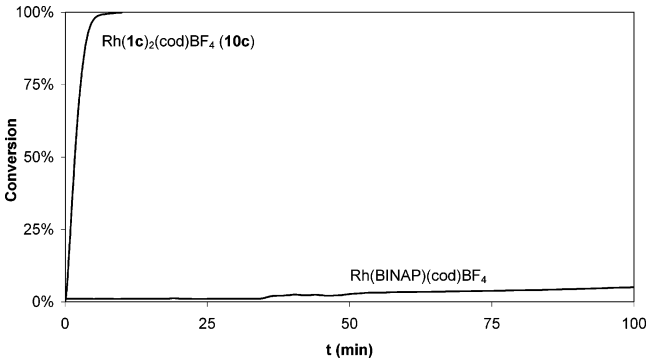

Figure 2. Comparison of hydrogenation of **7** using $Rh(\mathbf{1c})_2(cod)BF_4$ (**10c**) in CH_2Cl_2 and Rh(BINAP)(cod)BF_4 in CH_3OH.

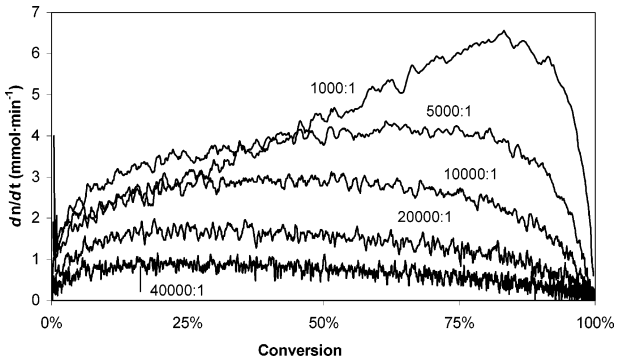

Figure 3. Rate of hydrogenation of **7** using $Rh(\mathbf{1h})_2(cod)BF_4$ (**10h**) at different S/C ratios.

It is well known that, in traditional precatalyst systems of the type $Rh(L)_2(cod)BF_4$, the active form is formed by hydrogenation of cod,[7−10,22,23] a process which provides coordination sites for the actual substrate. To study this aspect in our system, we investigated the influence of the substrate-to-catalyst ratio (S/C), keeping the initial substrate concentration identical. This was performed in the hydrogenation of **7** using the benzyl phosphite-derived catalyst $Rh(\mathbf{1h})_2(cod)BF_4$ (**10h**). Reaction rate, calculated as the derivative of the H_2 uptake (pressure drop) with respect to time (mmol·min^{-1}), was plotted as a function of conversion (Figure 3).

It can be seen that, at a S/C ratio of 1000:1, the reaction rate increases continuously and reaches a maximum at 83% conversion. This suggests that, at relatively high catalyst loading, the

(20) See for example: (a) Hannen, P.; Militzer, H.-C.; Vogl, E. M.; Rampf, F. A. *Chem. Commun. (Cambridge, U.K.)* **2003**, 2210−2211. (b) Chen, W.; Xiao, J. *Tetrahedron Lett.* **2001**, *42*, 2897−2899. (c) Huang, H.; Zheng, Z.; Luo, H.; Bai, C.; Hu, X.; Chen, H. *J. Org. Chem.* **2004**, *69*, 2355−2361. (d) Jerphagnon, T.; Renaud, J.-L.; Demonchaux, P.; Ferreira, A.; Bruneau, C. *Adv. Synth. Catal.* **2004**, *346*, 33−36. (e) Hua, Z.; Vassar, V. C.; Ojima, I. *Org. Lett.* **2003**, *5*, 3831−3834.

(21) Meiswinkel, A. Dissertation, Ruhr-Universität Bochum, Germany, 2003.

(22) (a) Sun, Y.; Landau, R. N.; Wang, J.; LeBlond, C.; Blackmond, D. G. *J. Am. Chem. Soc.* **1996**, *118*, 1348−1353. (b) Sun, Y.; Wang, J.; LeBlond, C.; Reamer, R. A.; Laquidara, J.; Sowa Jr, J. R.; Blackmond, D. G. *J. Organomet. Chem.* **1997**, *548*, 65−72.

(23) (a) Heller, D.; Kortus, K.; Selke, R. *Liebigs Ann. Chem.* **1995**, 575−581. (b) Heller, D.; Borns, S.; Baumann, W.; Selke, R. *Chem. Ber.* **1996**, *129*, 85−89. (c) Börner, A.; Heller, D. *Tetrahedron Lett.* **2001**, *42*, 223−225. (d) Drexler, H. J.; Baumann, W.; Spannenberg, A.; Fischer, C.; Heller, D. *J. Organomet. Chem.* **2001**, *621*, 89−102.

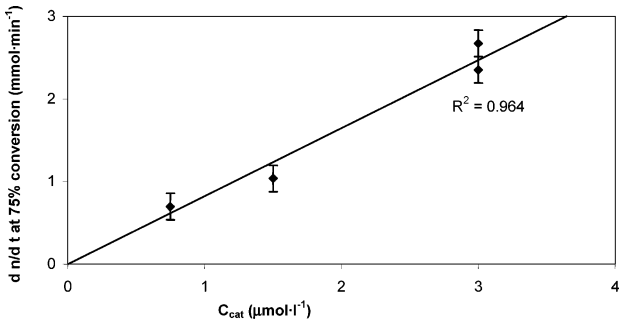

Figure 4. Influence of catalyst concentration on the hydrogenation of **7** using Rh(**1h**)$_2$(cod)BF$_4$ (**10h**) as catalyst.

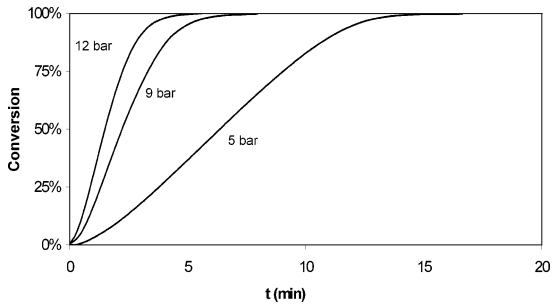

Figure 5. Influence of pressure on the hydrogenation of **7** using Rh(**1h**)$_2$(cod)BF$_4$ (**10h**) as catalyst.

hydrogenative cleavage of cod acts to increase catalyst concentration over a significant portion of the reaction, a phenomenon that Heller et al. demonstrated previously in other cases involving chiral diphosphines as ligands.[23] We observed a qualitatively similar trend at a S/C ratio of 5000:1. In this case, the maximum is reached at about 65% conversion. At still lower S/C ratios, the reaction rate does not rise but appears to be close to zero order in substrate over the course of the reaction.

More concise information emerges when the reaction rate is plotted against the catalyst concentration at a given conversion, e.g., 75% (Figure 4). At low catalyst loading ($c_{cat} < 3\ \mu mol \cdot L^{-1}$, corresponding to S/C > 10000:1), a linear relationship between the rate at 75% conversion and the catalyst concentration holds. This suggests that, at high S/C ratios and high conversions, a significant overlap of catalyst activation and substrate hydrogenation can be excluded. All further kinetic experiments were therefore performed at S/C ratios between 10000:1 and 50000:1.

To study the possible influence of pressure, hydrogenation of **7** was performed at 5, 9, and 12 bar using the benzyl phosphite-derived catalyst Rh(**1h**)$_2$(cod)BF$_4$ (**10h**). Figure 5 clearly shows that the rate of hydrogenation depends linearly upon the H_2 pressure, which can be viewed as evidence that oxidative addition of H_2 is the rate-determining step. Halpern,[9] Brown,[10] Noyori,[7,24] Landis,[11] and others[8] have previously reached the same conclusion in other Rh-catalyzed olefin hydrogenation reactions (diphosphine ligand systems). The linearity of the conversion vs time plots also implies strong binding of the substrate (saturation kinetics). Of theoretical and practical significance is our observation that the enantioselectivity of the reaction remains constant in the pressure range of 1.3−12 bar (ee = 98.0 ± 0.2%). The same applies when other

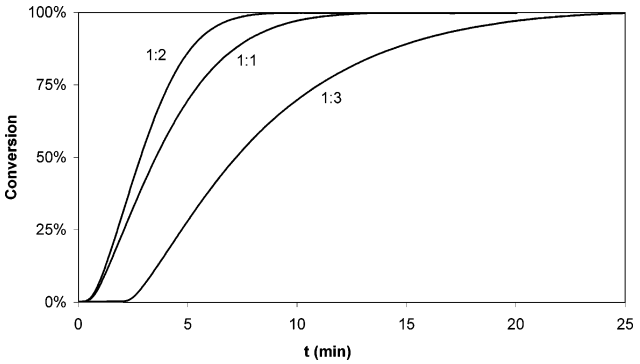

Figure 6. Influence of the Rh:**1h** ratio on the hydrogenation of **7** using Rh(**1h**)$_2$(cod)BF$_4$ (**10h**) as the catalyst.

BINOL-derived phosphites are employed, such as the isopropyl derivative **1c** (ee = 97.6% at 1.3 bar; 96.0% (20 bar); 96.0% (50 bar); 95.2% (100 bar)). In contrast, in some diphosphine-based systems, the ee decreases significantly at high pressures.[10,24]

To define the optimal Rh/ligand ratio, the kinetics of the hydrogenation of **7** using the isopropyl phosphite-derived catalyst Rh(**1c**)$_2$(cod)BF$_4$ (**10c**) was studied at a substrate/Rh ratio of 20000:1. Figure 6 demonstrates that a Rh/ligand ratio of 1:2 is optimal. This is also the case when other monodentate phosphites, such as **1h**, are used in the hydrogenation. The results are in line with the postulate that the catalytically active species has two phosphite ligands bonded to rhodium. At a 1:1 ratio, only part of the rhodium is stabilized as RhL_2, a portion probably forming a Rh colloid with much lower hydrogenation activity.[21] In contrast, a 1:3 ratio leads to an extended induction period and lowers activity, suggesting that excess phosphite begins to block free coordination sites necessary for substrate hydrogenation. Thus, our results are different from those of Zhou et al., who postulated that, in Rh-catalyzed olefin hydrogenation using a monodentate phosphoramidite based on a chiral spirodiol, only one such P-ligand is bonded to the metal in the active species.[25] In a preliminary mechanistic study by Minnaard, Feringa, and de Vries concerning Rh-catalyzed olefin hydrogenation using phosphoramidite **3**, no clear conclusion was reached regarding the number of ligands at the metal in the active species.[19b]

How do monophosphites **1**, monophosphonites **2**, and monophosphoramidites such as **3** compare in terms of catalyst activity? This aspect was studied by performing the hydrogenation of **7** using Rh(**1c**)$_2$(cod)BF$_4$, Rh(**2**)$_2$(cod)BF$_4$, (R = CH$_3$), and Rh(**3**)$_2$(cod)BF$_4$. Figure 7 shows that the phosphonite constitutes the most active system, followed by the phosphite, whereas the phosphoramidite leads to the least reactive catalyst system. The S-shape of the conversion vs time curve for the phosphoramidite suggests that catalyst activation competes with hydrogenation for a significant portion of the reaction for this catalyst. Of course, other BINOL-derived phosphoramidites may show different catalytic profiles, depending upon the nature of the substituents at nitrogen. For example, the piperidino analogue of **3** leads to higher activity and enantioselectivity than the parent dimethylamino ligand.[18b,19d]

The question whether rate differences occur within the phosphite series was also addressed.[21] Accordingly, the kinetics

(24) (a) Noyori, R. *Asymmetric Catalysis in Organic Synthesis*; John Wiley & Sons: New York, 1994. (b) Noyori, R. *Chem. Soc. Rev.* **1989**, *18*, 187−208. (c) Noyori, R. *Acta Chem. Scand.* **1996**, *50*, 380−390.

(25) Fu, Y.; Guo, X.-X.; Zhu, S.-F.; Hu, A.-G.; Xie, J.-H.; Zhou, Q.-L. *J. Org. Chem.* **2004**, *69*, 4648−4655.

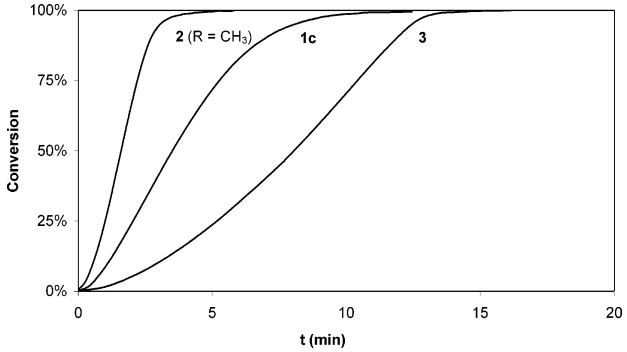

Figure 7. Comparison of Rh(**1c**)$_2$(cod)BF$_4$ (**10c**), Rh(**2**)$_2$(cod)BF$_4$ with R = CH$_3$, and Rh(**3**)$_2$(cod)BF$_4$ as catalysts in the hydrogenation of **7**.

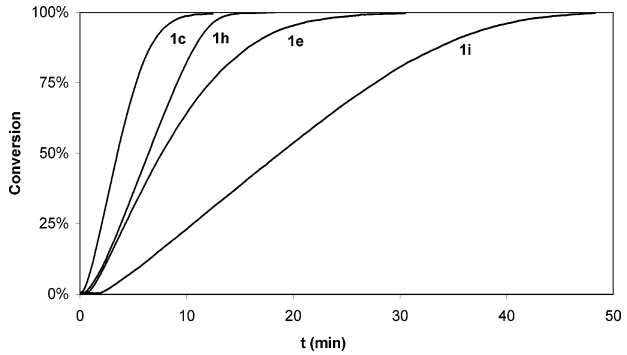

Figure 8. Comparison of Rh(**1c**)$_2$(cod)BF$_4$ (**10c**), Rh(**1e**)$_2$(cod)BF$_4$ (**10e**), Rh(**1h**)$_2$(cod)BF$_4$ (**10h**), and Rh(**1i**)$_2$(cod)BF$_4$ (**10i**) as catalysts in the hydrogenation of **7**.

of the hydrogenation of **7** was studied using four selected ligands, **1c**, **1e**, **1h**, and **1i**. The results show that catalyst activity decreases in the series **1c** > **1h** > **1e** > **1i** (Figure 8). Whereas the isopropyl and benzyl derivatives give complete conversion within 10−13 min, the neopentyl phosphite requires 30 min for completion, its lower activity possibly resulting from steric effects. The least reactive catalyst system is derived from the methoxyethyl phosphite **1i**, which may be due to the electron-withdrawing effect of the methoxy moiety.

Nonlinear Effects

Following the pioneering work of Kagan,[26] demonstrating nonlinear effects (NLE) of catalyst enantiopurity on product enantiomeric excess, studies of non-enantiomerically pure catalysts have become a diagnostic tool for probing the nature of catalyst species in asymmetric catalytic reactions.[27,28] The observation of an NLE indicates that species containing two (or more) chiral ligands either are involved in the transition state of the reaction[26] or exist outside the catalytic cycle.[27a] NLEs in hydrogenation reactions appear to be rare.[27d,e] In the present case, we studied the Rh-catalyzed hydrogenation of itaconate **7** using the isopropyl-derived phosphite **1c** as ligand.

Kagan's ML$_2$ model considers the case where three species containing two ligands each may be formed, namely ML^{R}L^R, ML^{S}L^S, and ML^{R}L^S, which are in equilibrium with one another (eq 1).[26]

$$\mathrm{ML^RL^R} + \mathrm{ML^SL^S} \rightleftharpoons 2\mathrm{ML^RL^S} \tag{1}$$

Upon reaction of racemic **1c** (two parts) with Rh(cod)$_2$BF$_4$ (one part), a 1:1:1.6 mixture of Rh(*R*-**1c**)$_2$(cod)BF$_4$, Rh(*S*-**1c**)$_2$-(cod)BF$_4$, and Rh(*R*-**1c**)/(*S*-**1c**)(cod)BF$_4$ was formed, as shown by its ^{31}P NMR spectrum. These species are precatalysts, since cod has to be removed from the complex by hydrogenation before the actual olefin hydrogenation can begin. The relative amounts of ML^{R}L^R, ML^{S}L^S, and ML^{R}L^S may well change on going from the precatalyst (characterized by NMR spectroscopy) to the active catalyst. Unfortunately, it was not possible to characterize the latter.

The ML$_2$ model assumes that these three species are in thermodynamic equilibrium (eq 1), their respective ratio being *x*:*y*:*z*, with an equilibrium constant equal to $K = z^2/(xy)$. The species ML^{R}L^R and ML^{S}L^S, whatever their exact structure may be, are enantiomeric and therefore exhibit identical activity as catalysts and give products with opposite configuration. The heterochiral species ML^{R}L^S may have different catalytic activity and gives racemic product. If ML^{R}L^S is less active than the homochiral species ML^{R}L^R and ML^{S}L^S, a positive NLE can be expected, whereas a negative NLE will result if ML^{R}L^S is more active. The factor *g* describes the relative activity of homochiral and meso species (eq 2):

$$k_{RS} = gk_{RR} = gk_{SS} \tag{2}$$

The ee of the product can therefore be described by eq 3, where ee$_0$ is the ee of the product obtained by an enantiopure catalyst.

$$\mathrm{ee_{prod}} = \mathrm{ee_0}\ \mathrm{ee_{cat}}\frac{1+\beta}{1+g\beta} \tag{3}$$

The parameter β is defined as the ratio of the heterochiral species to the sum of the homochiral species and may be given in terms of the catalyst ee, ee$_{cat}$, and the equilibrium constant, *K*:

$$\beta = \frac{z}{x+y} = \frac{-K\ \mathrm{ee_{cat}}^2 + \sqrt{-4K\ \mathrm{ee_{cat}}^2 + K(4 + K\ \mathrm{ee_{cat}}^2)}}{4 + K\ \mathrm{ee_{cat}}^2} \tag{4}$$

The Rh-catalyzed hydrogenation of olefin **7** using ligand **1c** is characterized by a positive NLE (Figure 9).[18c,21] The experimental curve can be modeled well by assuming the ML$_2$ model in which $K = 4$ and $g = 0$. This represents the special case in which the three species are formed stochastically and the heterochiral species is inactive as a catalyst.

A statistical distribution of active species ($K = 4$) implies that formation of ML^{R}L^S is not energetically favored or disfavored over formation of ML^{R}L^R (or ML^{S}L^S). It is thus unambiguously clear that the active species cannot be of the

(26) (a) Puchot, C.; Samuel, O.; Dunach, E.; Zhao, S.; Agami, C.; Kagan, H. B. *J. Am. Chem. Soc.* **1986**, *108*, 2353−2357. (b) Girard, C.; Kagan, H. B. *Angew. Chem.* **1998**, *110*, 3088−3127; *Angew. Chem., Int. Ed.* **1998**, *37*, 2923−2959. (c) Guillaneux, D.; Zhao, S.-H.; Samuel, O.; Rainford, D.; Kagan, H. B. *J. Am. Chem. Soc.* **1994**, *116*, 9430−9439.

(27) See also: (a) Kitamura, M.; Okada, S.; Suga, S.; Noyori, R. *J. Am. Chem. Soc.* **1989**, *111*, 4028−4036. (b) Yamakawa, M.; Noyori, R. *J. Am. Chem. Soc.* **1995**, *117*, 6327−6335. (c) Noyori, R.; Kitamura, M. *Angew. Chem.* **1991**, *103*, 34−55; *Angew. Chem., Int. Ed. Engl.* **1991**, *30*, 49−69. (d) Girard, C.; Genêt, J.-P.; Bulliard, M. *Eur. J. Org. Chem.* **1999**, 2937−2942. (e) Faller, J. W.; Mazzieri, M. R.; Nguyen, J. T.; Parr, J.; Rokunaga, M. *Pure Appl. Chem.* **1994**, *66*, 1463−1469.

(28) (a) Blackmond, D. G. *J. Am. Chem. Soc.* **1997**, *119*, 12934−12939. (b) Blackmond, D. G. *J. Am. Chem. Soc.* **1998**, *120*, 13349−13353. (c) Blackmond, D. G. *Acc. Chem. Res.* **2000**, *33*, 402−411. (d) Blackmond, D. G. *J. Am. Chem. Soc.* **2001**, *123*, 545−553. (e) Blackmond, D. G.; McMillan, C. R.; Ramdeehul, S.; Schorm, A.; Brown, J. M. *J. Am. Chem. Soc.* **2001**, *123*, 10103−10104.

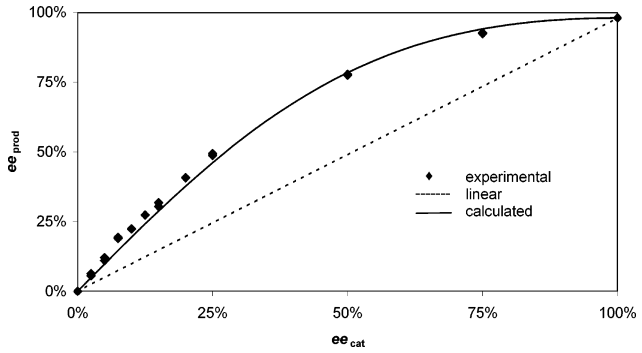

Figure 9. Nonlinear effects (NLEs) in the hydrogenation of **7** using Rh-(**1e**)$_2$(cod)BF$_4$ (**10e**) as the catalyst.

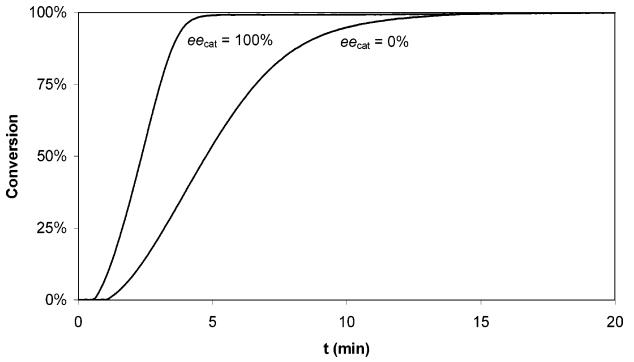

Figure 10. Comparison of enantiomerically pure **1c** and racemic **1c** as ligands in the Rh-catalyzed hydrogenation of **7**.

type ML having only one phosphite ligand, with higher order species contained in a reservoir off the catalytic cycle. If such a reservoir effect were in operation, then dissociation of all ML_2 species with formation of ML would occur to the same extent, the result being that the ee arising from ML would be identical to the ee of the ligand. This is not observed, and we therefore conclude that, in the transition state of hydrogenation, two P-ligands **1** are bonded to rhodium. In the case of hydrogenation using phosphoramidite **3**, Minnaard, Feringa, and de Vries also observed a positive NLE, but no unambiguous mechanistic conclusions were made.[19b] In the case of the spiro-phosphoramidite described by Zhou and co-workers, a positive NLE was likewise observed, but they suggested that only one ligand is bound to the active catalyst.[25] Although they did not calculate K values for the ML_2 or the reservoir model, their data suggest that their system also exhibits close to the statistical distribution of homochiral and heterochiral species. As we note above, observation of a statistical distribution of species precludes a one-ligand active catalyst system.

In addition to describing the enantioselectivity on the basis of the ML_2 model, it is also possible to predict the relative rates as a function of ee_{cat}. Blackmond[28] has shown that the parameter K may also be used to determine the distribution of species at any ee_{cat}. The rate of reaction expected for a catalyst of ee_{cat} may therefore be determined from this distribution and the parameter g, as shown in eq 5.

$$\frac{\text{rate(scalemic)}}{\text{rate(enantiopure)}} = (x + y + gz) \qquad \text{where } (x + y + z) = 1 \quad (5)$$

In a racemic mixture of ligands L^R and L^S exhibiting a statistical distribution of ML_2 species, the ratio of species (x:y:z) in fractional terms is equal to (0.25:0.25:0.5), showing that 50% of the catalyst will be present as the meso complex ML^RL^S. When $g = 0$, eq 5 thus shows that the total active Rh catalyst concentration will be reduced by 50% compared to that in an enantiopure mixture. To confirm this conclusion, the kinetics of the Rh-catalyzed hydrogenation of **7** was studied using racemic ligand **1c**. Control experiments employing a pressure of 5 bar (H_2) and a substrate-to-catalyst ratio of 50000:1 showed that the same NLEs occur as before. Therefore, all kinetic experiments were performed under these conditions.[21] As expected, strikingly different rates were observed upon using enantiomerically pure **1c** on one hand and the racemate on the other. The reaction employing pure (*R*)-**1c** is over within 5 min (Figure 10), whereas the use of *rac*-**1c** under the same conditions results in only 50% conversion, in excellent agreement with the model prediction.

Theoretical Studies

One of the first steps in the generally accepted catalytic cycle of the Rh-catalyzed asymmetric hydrogenation of prochiral olefins is the complexation of the substrate to the precatalyst Rh(L)$_2$(cod)BF$_4$.[7−11,24] Of course, as stated above, the cod ligand has to be cleaved first in order to generate an active catalyst. Coordination of the pro-*R* and pro-*S* sides of the olefin then leads to diastereomeric Rh complexes. In the case of traditional C_2-symmetric diphosphines, two diastereomers are involved, namely the major and the minor intermediates (Halpern nomenclature).[9] The assumption that the hydrogen arrives from the side of the metal and therefore dictates the stereochemical outcome in each case is generally accepted.[5−10] In the present study, the situation is more complicated because two monodentate ligands are involved. Hence, C_2-symmetry no longer holds, and consequently *four* different cationic catalyst-substrate adduct complexes [Rh(L)$_2$(olefin)]$^+$ (two diastereomer pairs) can be formed (Figure 11). In each pair, the metal coordinates with one enantioface of the prochiral olefin (pro-*R* or pro-*S*). If conformational differences are considered, which may arise from changes in the catalyst framework, i.e., rotations around the Rh−L bond, then additional species need to be considered (see below).

As pointed out above, according to Halpern, the predominant enantiomer of the product in classical diphosphine systems arises from the minor (less stable) diastereomer of the catalyst-substrate adduct (anti lock-and-key concept) by virtue of its much higher reactivity toward H_2.[9] This concept was verified experimentally, inter alia by the predicted and observed reduction (and inversion) of the enantioselectivity with increasing hydrogen pressure.[5−10,24] Theoretical studies by Landis and co-workers,[11] who performed three-layer ONIOM calculations on smaller systems with chelating P-ligands, are in line with the experimental results. They point to the barrier for the oxidative addition of hydrogen from the five-coordinated molecular hydrogen complex to the six-coordinated pseudo-octahedral alkyl hydride complex as the rate-determining step of the catalytic cycle.[11] While these results were obtained using rigid bidentate P-ligands, the ligands in our system consist of two monodentate P-ligands, which in principle should allow for a higher flexibility of the catalyst framework. Nevertheless, comparably high enantioselectivities were obtained experimen-

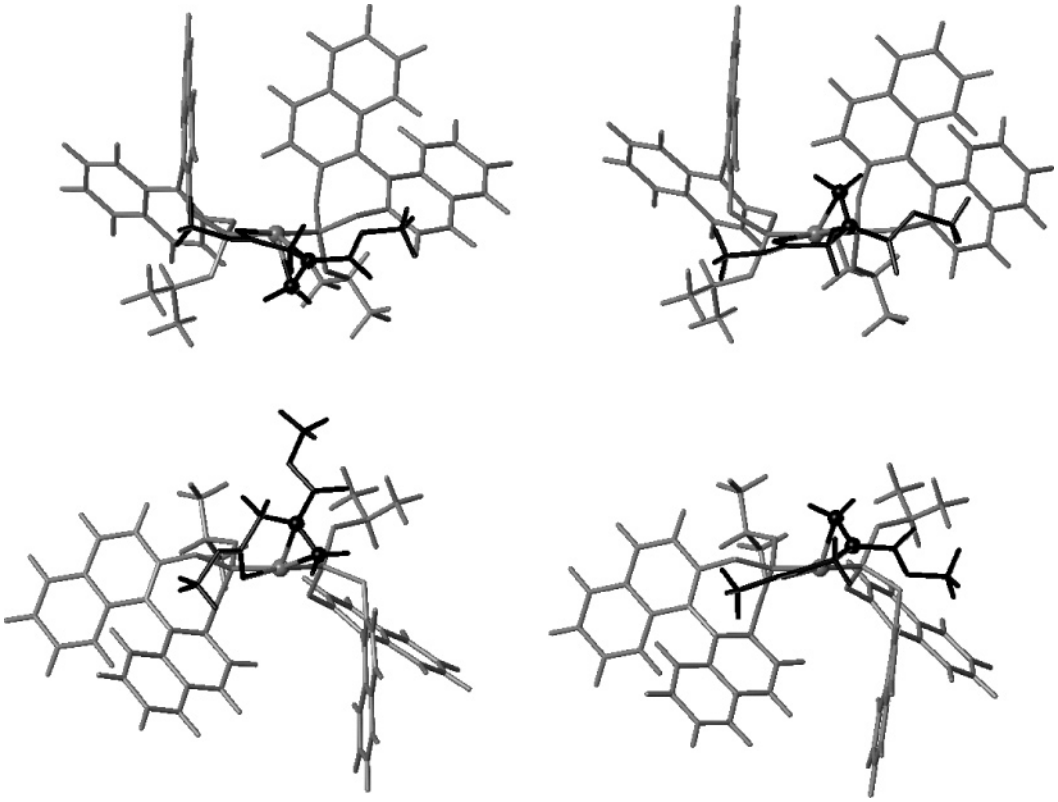

Figure 11. Coordination modes of olefin **7** with [Rh(**1c**)$_2$]$^+$. (Left) Two conformers involving pro-*S* complexation. (Right) Two conformers involving pro-*R* complexation.

tally. Therefore, the prime goal of the theoretical study was to explain the source of enantioselectivity using DFT calculations.

All calculations refer to the Rh-catalyzed hydrogenation of itaconic acid dimethyl ester (**7**) using the monophosphite **1c** as the ligand L. This particular ligand was chosen because of its optimal combination of ligand size, ligand flexibility, and enantiomeric excess obtained (Table 1). Only the enantiopure system [Rh(**1c**)$_2$(olefin)]$^+$ with *R* configuration of the phosphite **1c** is considered in this paper. We plan to use it as a reference in later analyses of systems containing ligands of different chirality and/or different chemical constitution. To ensure an accurate treatment of the chemical problem, unconstrained DFT calculations of the full system were preferred over a computationally faster combined quantum mechanical/molecular mechanical approach.

Six torsion angles (θ_1, P2−Rh−P1−O2; θ_2, P2−Rh−P1−O1; θ_3, Rh−P1−O1−C1; θ_4, Rh−P2−O2−C2; θ_5, P1−O1−C1−H1; θ_6, P2−O2−C2−H2) mainly contribute to the conformational flexibility of the catalyst framework of [Rh(**1c**)$_2$(olefin)]$^+$ (Figure 12). Within an energy range of 4 kcal/mol (ΔE), seven different conformations (local minima) of the pro-*R* adduct (ADD-*R*-A to ADD-*R*-G) and five different conformations of the pro-*S* adduct (ADD-*S*-A to ADD-*S*-E) could be located (Table 2). The superposition of all 12 conformers (Figure 13) reveals an appreciable degree of flexibility of the catalyst framework. Most remarkably, three different pro-*R* conformers (ADD-*R*-A, ADD-*R*-B, ADD-*R*-C) are of lower energy than the lowest pro-*S* conformer (ADD-*S*-A), although experimentally the *R*-enantiomer is obtained with 98% ee. Thus, in our system the reaction does not follow the anti lock-and-key concept proposed by Halpern for rigid chelating diphosphine systems. Rather, it obeys the lock-and-key principle. The free energy

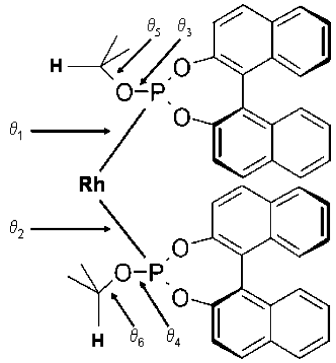

Figure 12. Catalyst framework of [Rh(**1c**)$_2$(olefin)]$^+$.

Table 2. Calculated Energies ΔE and Dihedral Angles θ_i (see Figure 12) of 12 Low-Energy Adduct Conformers

[Rh(**1c**)$_2$(olefin)]$^+$	ΔE (kcal/mol)	θ_1 (deg)	θ_2 (deg)	θ_3 (deg)	θ_4 (deg)	θ_5 (deg)	θ_6 (deg)
ADD-*R*-A	0.0	96	−46	167	−177	12	13
ADD-*R*-B	0.1	124	−35	178	165	13	21
ADD-*R*-C	0.3	97	−37	178	156	14	19
ADD-*R*-D	2.6	−59	100	177	158	14	19
ADD-*R*-E	2.6	−60	−41	175	−176	17	15
ADD-*R*-F	3.5	−58	102	163	159	15	18
ADD-*R*-G	3.9	155	125	179	164	15	15
ADD-*S*-A	1.4	−73	−56	170	166	19	17
ADD-*S*-B	1.6	−77	107	171	158	18	19
ADD-*S*-C	2.5	82	−40	166	180	22	13
ADD-*S*-D	2.6	108	−66	164	179	22	13
ADD-*S*-E	3.7	92	100	161	155	23	20

difference ($\Delta\Delta G_{298}$) between the lowest pro-*S* and the lowest pro-*R* adduct conformations (Figure 14) amounts to 2.2 kcal/mol, almost the same as the value for the free energy difference $\Delta\Delta G^{\ddagger}_{298}$ between the rate-determining reaction steps deduced from the experimentally observed enantiomeric excess.

Figure 13. Superposition of the 12 low-energy conformers of [Rh(**1c**)$_2$(olefin)]$^+$. The coordinated olefin **7** has been omitted for clarity.

At this stage, the theoretical study is incomplete, because the transition states at every stage of the catalytic cycle have not been considered. This requires extensive DFT calculations, which are currently in progress. However, the initial DFT results presented here clearly show that the major diastereomer leads to the experimentally observed enantiomer, a conclusion that is independent of the relative energies of all transition states that follow in the catalytic cycle.

Conclusions

BINOL-derived monodentate phosphites of the type **1** have emerged as cheap, easily accessible, and efficient ligands for Rh-catalyzed olefin hydrogenation.[15,18,20] Thus far, five different classes of olefins have been hydrogenated successfully (90−99% ee) using these ligands: itaconate-type substrates such as **7**, α-acylamino acrylic acid esters, *β*-acylamino acrylic acid esters, *N*-acyl enamides, and enol carboxylates. Currently, it is difficult to predict which particular derivative of **1** is optimal for a given substrate, which means that an empirical approach is necessary. Nevertheless, the present study has unveiled the basic facets of the mechanism. First, based on the kinetics, nonlinear effects, and NMR data, it is certain that two monodentate ligands **1** are attached to the metal. Second, DFT calculations strongly suggest that the system obeys the lock-and-key mechanism not found in the original Rh-catalyzed hydrogenations using chiral diphosphines as reported by Halpern.[9] The thermodynamics of diastereoselective *π*-complexation of the prochiral olefin with formation of the minor and major intermediates dictates the stereochemical outcome; i.e., the major isomer leads to the observed configuration of the product. Strictly speaking, this conclusion pertains to the substrate (**7**) considered in this study; i.e., other substrates may behave differently. Further DFT studies on the complete catalytic cycle are in progress. Finally, the combinatorial hydrogenation method based on the use of two different monodentate P-ligands also needs to be studied mechanistically.[29]

Experimental Section

General Remarks. NMR spectra were recorded on Bruker Avance-400 spectrometers. ^{31}P NMR chemical shifts are given relative to external 85% aqueous phosphoric acid. ^{1}H and ^{13}C chemical shifts were determined relative to the solvent signals and converted to the TMS scale [$\delta_H(CHCl_3) \equiv 7.24$, $\delta_C(CDCl_3) \equiv 77.0$; $\delta_H(CHDCl_2) \equiv 5.32$,

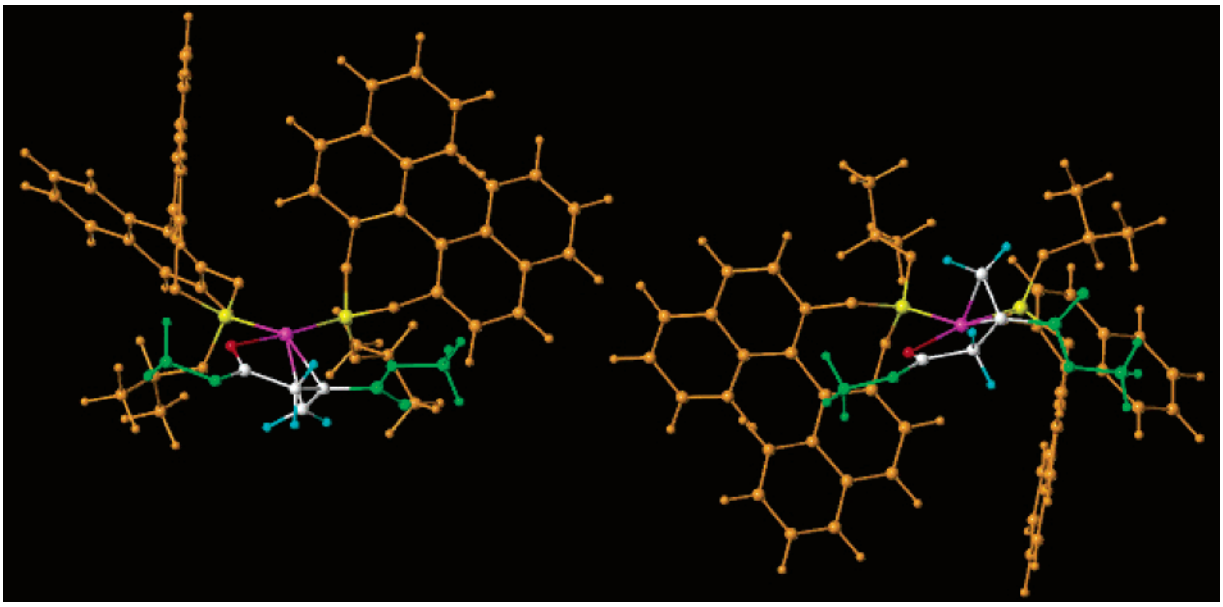

Figure 14. Lowest energy pro-*S* and pro-*R* conformers of [Rh(**1c**)$_2$(olefin)]$^+$, the olefin being **7**. (Left) ADD-*S*-A ($\Delta G_{298} = 2.2$ kcal/mol). (Right) ADD-*R*-A ($\Delta G_{298} = 0$ kcal/mol). Color code: catalyst framework uniformly brown with P yellow and Rh magenta; C white, H cyan, and O red in central part of olefin; outer parts of olefin uniformly green.

$\delta_C(CD_2Cl_2 \equiv 53.8]$. The signal assignments for **1e** and **10e** were achieved using a combination of 2D NMR spectra (COSY, HMQC, and HMBC) with the multiplet structures in the ^{1}H NMR spectrum. Itaconic acid dimethyl ester (**7**) was purchased from Fluka or Acros and distilled prior to use. (*R*)- and (*S*)-BINOL were purchased from Reuter Chemische Apparate KG, Freiburg, Germany. BINOL-derived phosphites were prepared according to literature procedures.[15,30] [Rh(cod)$_2$]BF$_4$ (**9**) was prepared according to a literature procedure.[31] Dichloromethane was dried and distilled over CaH_2. All operations were performed under argon. All vessels and autoclaves were heated, evacuated, and filled with argon three times.

NMR data for 1e: ^{1}H NMR ($CDCl_3$, 400.1 MHz) δ 8.02 (d, J_{HH} = 8.8 Hz, 1 H, H4/H4′), 7.98 (d, J_{HH} = 8.9 Hz, 1 H, H4/H4′), 7.96 (d, J_{HH} = 8.7 Hz, 1 H, H5/H5′), 7.95 (d, J_{HH} = 8.7 Hz, 1 H, H5/H5′), 7.53 (d, J_{HH} = 9.1 Hz, 1 H, H3/H3′), 7.47 (m, 1 H, H6/H6′), 7.45 (d, J_{HH} = 8.6 Hz, 1 H, H3/H3′), 7.44 (m, 1 H, H6/H6′), 7.35 (d, J_{HH} = 8.3 Hz, 1 H, H8/H8′), 7. 34 (d, J_{HH} = 8.9 Hz, 1 H, H8/H8′), 7.28 (t, J_{HH} = 7.6 Hz, 1 H, H7/H7′), 7.27 (t, J_{HH} = 7.6 Hz, 1 H, H7/H7′), 3.69 (dd, J_{PH} = 7.3 Hz, J_{HH} = 7.2 Hz, 1 H, H9a), 3.50 (dd, J_{PH} = 7.0 Hz, J_{HH} = 7.0 Hz, 1 H, H9b), 0.92 (s, 9 H, H); ^{13}C NMR ($CDCl_3$, 100.6 MHz) δ 149.2 (d, J_{PC} = 5.6 Hz, C2/C2′), 148.0 (d, J_{PC} = 1.7 Hz, C2/C2′) 133.2 (d, J_{PC} = 1.4 Hz, C8a/C8a′), 132.9 (C8a/C8a′), 132.0 (C4a/C4a′), 131.5 (C4a/C4a′), 130.8 (C4/C4′), 130.3 (C4/C4′), 128.79 (C5/C5′), 128.75 (C5/C5′) 127.17 (C8/C8′), 127.14 (C8/C8′), 126.65 (C7/C7′), 126.59 (C7/C7′), 125.44 (C6/C6′), 125.26 (C6/C6′), 124.51 (d, J_{PC} = 5.4 Hz, C1/C1′), 123.03 (d, J_{PC} = 2.7 Hz, C1/C1′), 122.2 (2 C, C3/C3′), 75.1 (d, J_{PC} = 7.2 Hz, C9), 32.5 (d, J_{PC} = 4.8 Hz, C10), 26.3 (3 C, C11); ^{31}P NMR ($CDCl_3$, 162 MHz) δ 143.3 (s).

NMR data for 10e: ^{1}H NMR (CD_2Cl_2, 400.1 MHz) δ 8.25 (d, J_{HH} = 8.6 Hz, 2 H, H4/H4′), 8.11 (d, J_{HH} = 8.6 Hz, 2 H, H4/H4′), 8.10 (d, J_{HH} = 8.6 Hz, 2 H, H5/H5′), 8.02 (d, J_{HH} = 8.6 Hz, 2 H, H5/H5′), 7.89 (d, J_{HH} = 8.6 Hz, 2 H, H3/H3′), 7.58 (t, J_{HH} = 7.0 Hz, 2 H, H6/H6′), 7.54 (t, J_{HH} = 6.5 Hz, 2 H, H6/H6′), 7.51 (d, J_{HH} = 8.0 Hz, 2 H, H3/H3′), 7.38 (t, J_{HH} = 8.1 Hz, 2 H, H7/H7′), 7.37 (d, J_{HH} = 10.1 Hz, 2 H, H8/H8′), 7.35 (d, J_{HH} = 10.6 Hz, 2 H, H8/H8′), 7.33 (t, J_{HH} = 8.1 Hz, 2 H, H7/H7′), 5.91 (s, 2 H, H12), 4.08 (s, 2 H, H12), 3.81 (d, J_{HH} = 9.6 Hz, 2 H, H9a), 3.73 (dt, J_{HH} = 9.6 Hz, $^1/_2(J_{PH} + J_{P'H})$ = 3.5 Hz, 2 H, H9b), 2.25 (2 H, H13), 2.10 (2 H, H13), 1.80 (2 H, H13), 1.10 (2 H, H13), 1.05 (s, 18 H, H11); ^{13}C NMR (100.6 MHz, CD_2Cl_2) δ 150.0 (d, $^1/_2(J_{PC} + J_{P'C})$ = 7.4 Hz, 2 C, C2/C2′), 146.2 (d, $^1/_2(J_{PC} + J_{P'C})$ = 2.2 Hz, 2 C, C2/C2′), 132.76 (2 C, C8a/C8a′), 132.64 (2 C, C8a/C8a′), 132.5 (2 C, C4a/C4a′), 131.9 (d, $^1/_2(J_{PC} + J_{P'C})$ = 4.8 Hz, 4 C, C4/C4′), 131.8 (2 C, C4a/C4a′), 129.0 (d, $^1/_2(J_{PC} + J_{P'C})$ = 4.8 Hz, 4 C, C5/C5′), 127.8 (2 C, C7/C7′), 127.6 (2 C, C8/C8′), 127.2 (2 C, C8/C8′), 127.2 (2 C, C7/C7′), 126.9 (2 C, C6/C6′), 126.4 (2 C, C6/C6′), 123.9 (2 C, C1/C1′), 121.5 (2 C, C3/C3′), 121.1 (2 C, C1/C1′), 120.2 (2 C, C3/C3′), 109.38 (2 C, C12), 109.13 (2 C, C12), 80.4 (d, $^1/_2(J_{PC} + J_{P'C})$ = 5.8 Hz, 2 C, C9), 32.7 (d, $^1/_2(J_{PC} + J_{P'C})$ = 2.9 Hz, 2 C, C10/C10′), 30.9 (2 C, C13), 28.8 (2 C, C13), 26.4 (6 C, C11); ^{31}P NMR (CD_2Cl_2, 162.0 MHz) δ 120.8 (d, J_{RhP} = 258 Hz).

In the ^{13}C and ^{1}H NMR spectra, the splittings due to phosphorus are apparent triplets. However, in the ^{13}C NMR isotopomers the phosphorus nuclei are magnetically inequivalent and the ^{13}C multiplets are the X part of ABX spin systems (A, B = ^{31}P, ^{31}P′). Since in such molecules $J_{PP'}$ must be considerably larger than the P,C couplings, the observed splittings are $^1/_2(J_{PC} + J_{P'C})$. Similarly, the observed splittings in the proton spectra are $^1/_2(J_{PH} + J_{P'H})$. The cod olefinic carbons are apparent quartets due to an additional coupling of the same magnitude with ^{103}Rh.

Kinetic Experiments. To ensure high reproducibility in kinetic experiments, the following procedure was applied (which is different from the synthetic procedure). In a typical experiment, 4.75 g (30 mmol) of itaconic acid dimethyl ester (**7**) was dissolved in about 80 mL of dichloromethane. The catalyst was added using 2 mM stock solutions of [Rh(cod)$_2$]BF$_4$ (**9**) and 2 equiv of the ligand or preformed Rh complexes [Rh(L)$_2$(cod)]BF$_4$ (**10**). The **7**/Rh ratio was fixed as desired, typically at 20000:1. The total volume was filled up to exactly 100 mL and then transferred into an autoclave (V4A stainless steel, 200 mL) with a gas injection stirrer. This reaction vessel was placed into a water bath, which was kept at constant temperature typically 20 °C. When isothermic conditions were reached (after about 30 min; temperature measured inside the autoclave), the autoclave was connected to a hydrogen reservoir using a reducing valve. The hydrogen pressure in the autoclave was typically set to 5 bar constant pressure. At the same moment, the stirrer and a clock were started, and the decrease of hydrogen pressure in the reservoir was recorded once every second using a computer with the program Quicklog PC v. 2.4.0 from Strawberry Tree Inc. The recorded pressure values were converted following the ideal gas equation. First, average pressure values over 10−30 s were taken, and the reaction speed was determined as the quotient $dp/dt = (p_1 - p_2)(t_1 - t_2)^{-1}$ in bar·min^{-1}. An average value over 5 s was calculated. For conversion of bar·min^{-1} into mmol·min^{-1}, these values were multiplied by a factor f [$f = n_{substrate}(p_{max} - p_{min})^{-1}$, where p_{max} is the highest pressure at the beginning of the reaction, i.e., at t_0, and p_{min} is the pressure at the end of the reaction]. Conversion was determined using the equation conversion = $(p - p_{min})(p_{max} - p_{min})^{-1}$. At the end of each experiment, a sample was investigated using GC analysis to check conversion and ee.

Computational Details. DFT calculations were performed using the Turbomole program package version 5.71,[32] employing the BP86 functional[33] with the RI approximation.[34] The basis set was 6-31G* [35] for all atoms, except for Rh, which was described by an effective core potential and the associated basis set (ecp-28-mwb).[36] The SCF convergence criterion was set to $10^{-7}E_h$. All systems were fully optimized in redundant internal coordinates without any constraints. Vibrational frequencies and thermodynamic properties were numerically calculated with SNF version 2.3.1c[37] on 16 processors in parallel, with an SCF convergence criterion of $10^{-8}E_h$.

Acknowledgment. This work was generously supported by the Fonds der Chemischen Industrie.

JA052025+

(29) (a) Reetz, M. T.; Sell, T.; Meiswinkel, A.; Mehler, G. *Angew. Chem.* **2003**, *115*, 814−817; *Angew. Chem., Int. Ed.* **2003**, *42*, 790−793. (b) Reetz, M. T.; Mehler, G. *Tetrahedron Lett.* **2003**, *44*, 4593−4596. (c) Reetz, M. T.; Mehler, G.; Meiswinkel, A.; Sell, T. *Tetrahedron: Asymmetry* **2004**, *15*, 2165−2167. (d) Reetz, M. T.; Meiswinkel, A.; Sell, T.; Mehler, G. Patent Appl. DE-A 10247633.0, 2002. (e) Reetz, M. T.; Li, X. *Angew. Chem.* **2005**, *117*, 3019−3021; *Angew. Chem., Int. Ed.* **2005**, *44*, 2959−2962. (f) See also: Peña, D.; Minnaard, A. J.; Boogers, J. A. F.; de Vries, A. H. M.; de Vries, J. G.; Feringa, B. L. *Org. Biomol. Chem.* **2003,** *1*, 1087−1089. (g) Duursma, A.; Hoen, R.; Schuppan, J.; Hulst, R.; Minnaard, A. J.; Feringa, B. L. *Org. Lett.* **2003**, *5*, 3111−3113.

(30) The synthesis of BINOL-derived monophosphites is well known:[15] (a) Ovchinnikov, V. V.; Cherkasova, O. A.; Verizhnikov, L. V. *Zh. Obshch. Khim.* **1982**, *52*, 707−708. (b) Bartik, T.; Gerdes, I.; Heimbach, P.; Schulte, H.-G. *J. Organomet. Chem.* **1989**, *367*, 359−370. (c) Heimbach, P.; Bartik, T.; Drescher, U.; Gerdes, I.; Knott, W.; Rienäcker, R.; Schulte, H.-G.; Tani, K. *Kontakte (Darmstadt)* **1988**, *3*, 19−31. (d) Fuji, K.; Kinoshita, N.; Tanaka, K.; Kawabata, T. *Chem. Commun. (Cambridge, U.K.)* **1999**, 2289−2290. (e) Tang, W.; Zhang, X. *Chem. Rev.* **2003**, *103*, 3029−3069.

(31) (a) Schenck, T. G.; Downes, J. M.; Milne, C. R. C.; Mackenzie, P. B.; Boucher, H.; Whelan, J.; Bosnich, B. *Inorg. Chem.* **1985**, *24*, 2334−2337. (b) Green, M.; Kuc, T. A.; Taylor, S. H. *J. Chem. Soc. A* **1971**, 2334−2337.

(32) Ahlrichs, R.; Bär, M.; Häser, M.; Horn, H.; Kölmel, C. *Chem. Phys. Lett.* **1989**, *162*, 165−169.

(33) (a) Becke, A. D. *Phys. Rev. A: At., Mol., Opt. Phys.* **1988**, 38, 3098−3100. (b) Perdew, J. P. *Phys. Rev. B: Condens. Mater. Phys.* **1986**, *33*, 8822−8824.

(34) (a) Eichkorn, K.; Treutler, O.; Öhm, H.; Häser, M.; Ahlrichs, R. *Chem. Phys. Lett.* **1995**, *242*, 652−660. (b) Eichkorn, K.; Weigend, F.; Treutler, O.; Ahlrichs, R. *Theor. Chem. Acc.* **1997**, *97*, 119−124.

(35) (a) Harihara, P. C.; Pople, J. A. *Theor. Chim. Acta* **1973**, *28*, 213−222. (b) Francl, M. M.; Pietro, W. J.; Hehre, W. J.; Binkley, J. S.; Gordon, M. S.; DeFree, D. J.; Pople, J. A. *J. Chem. Phys.* **1982**, *77*, 3654−3665.

(36) Andrae, D.; Häussermann, U.; Dolg, M.; Stoll, H.; Preuss, H. *Theor. Chim. Acta* **1990**, *77*, 123−141.

(37) Neugebauer, J.; Reiher, M.; Kind, C.; Hess, B. A. *J. Comput. Chem.* **2002**, *23*, 895−910.